

Three Baryon Interaction Generated by Determinant Interaction of Quarks[†]

Akira Ohnishi^{1,*}, Kouji Kashiwa^{1,†}, and Kenji Morita^{1,‡}

Yukawa Institute for Theoretical Physics, Kyoto University, Kyoto 606-8502, Japan

*E-mail: ohnishi@yukawa.kyoto-u.ac.jp, †kouji.kashiwa@yukawa.kyoto-u.ac.jp,

‡kmorita@yukawa.kyoto-u.ac.jp,

.....
 We discuss the three-baryon interaction generated by the determinant interaction of quarks, known as the Kobayashi-Maskawa-'t Hooft (KMT) interaction. The expectation value of the KMT interaction operator is calculated in fully-antisymmetrized quark-cluster model wave functions for one-, two- and three-octet baryon states. The three-baryon potential from the KMT interaction is found to be repulsive for NNA and $N\Lambda\Lambda$ systems, while it is zero for the NNN system. The strength and range of the three-baryon potential are found to be comparable to those for the NNN three-body potential obtained in lattice QCD simulations. The contribution to the Λ single particle potential in nuclear matter is found to be 0.28 MeV and 0.73 MeV in neutron matter and symmetric nuclear matter at normal nuclear density, respectively. These repulsive forces are not enough to solve the hyperon puzzle, but may be measured in high-precision hyperisotope experiments.

Subject Index D30, D00, D41

1. Introduction

The discovery of two-solar-mass neutron stars [1, 2] has cast doubt on the equation of state (EOS) based on conventional nuclear physics. EOSs with nucleons and leptons for neutron star matter can support neutron stars whose masses are $M \sim 2M_{\odot}$, where M_{\odot} is the solar mass. With hyperons (Y), however, the EOS generally becomes much softer and many of proposed EOSs cannot support $2M_{\odot}$ neutron stars [3–7]. This problem, referred to as the *hyperon puzzle*, has been attracting much attention.

Several mechanisms have been proposed so far to solve the hyperon puzzle. One of the ideas is to assume that the crossover transition [8, 9] from nuclear matter to quark matter takes place at relatively low density, $2 - 3\rho_0$, with $\rho_0 \simeq 0.16 \text{ fm}^{-3}$ being the normal nuclear matter density, instead of the often assumed first order deconfinement phase transition at high density. In this case, the transition may occur at lower density than the onset of hyperon mixing via the weak interaction, and then prevents the matter from softening owing to emergence of the hyperons. The crossover nature of the transition also circumvents the softening from the first order phase transition. This crossover picture can be examined by making use of high-energy heavy-ion collision experiments. Indeed, the direct flow collapse in Au+Au collisions at $\sqrt{s_{NN}} = 11.5 \text{ GeV}$ [10] seems to suggest the sudden softening of

[†]Report No: YITP-16-115

EOS [11], which could be caused by the first order phase transition. Further studies including the isospin asymmetry dependence of the phase transition order are necessary to examine the crossover transition in dense neutron-rich matter. Another idea is to modify the hyperon-nucleon (YN) interaction. Within the flavor $SU(3)$ coupling scheme but off the flavor-spin $SU(6)$ couplings, one can obtain a stiff hyperonic matter EOS [12] with parameters including large $\bar{s}s$ contents in nucleons, which however contradicts the recent lattice QCD calculations; see Ref. [13] and references therein. The third idea is to introduce the three-baryon ($3B$) interaction involving hyperons. If the three-nucleon ($3N$) force is repulsive and there exists repulsive $3B$ forces involving hyperons, the EOS can support the $2M_\odot$ neutron stars by suppressing the hyperon mixing at high densities.

The role of the $3N$ force has been extensively discussed in nuclear physics. Ab initio calculations with two-nucleon interactions cannot reproduce the binding energies of three-nucleon systems (t and ${}^3\text{He}$) and the nuclear matter saturation point, and it has been noticed that three-nucleon ($3N$) force is necessary to reproduce these fundamental aspects of nucleon many-body systems [14–21]. The $3N$ force contains two-pion P-wave exchange term with an intermediate Δ excitation (Fujita-Miyazawa force) [14] and shorter-range phenomenological term [15]. One of the physical pictures of the short-range $3N$ force is the multi-pomeron exchange [16]. Recently, $3N$ force has been derived systematically in the chiral effective field theory, where energy-independent $3N$ forces appear at the next-to-next-to-leading order [17, 18]. Microscopic calculations including these $3N$ forces show that the $3N$ force is relevant to the nuclear matter saturation and the nuclear matter EOS at high densities [15, 16, 19–21], and also to deuteron-proton scattering observables [22]. Moreover, there have been remarkable progress in the lattice QCD simulation for the $3N$ force based on the Nambu-Bethe-Salpeter wave function, i.e. HAL QCD method [23]. At present, such lattice QCD simulations have been performed for larger π masses than the physical π mass and then their data still have large error-bars. Cooperations between lattice QCD simulations, experiments and phenomenological approaches including present study should play an important role to understand nature of the $3N$ force and also other $3B$ forces in future.

So far $3B$ forces involving hyperons have not been known well. The currently available hypernuclear data are not enough to determine the $3B$ force involving hyperons precisely at the level of the $3N$ force, then we have to rely on some models or assumptions. In Ref. [16], the repulsive $3B$ forces are assumed to work universally for YNN , YYN , YYY as well as for NNN in the multi-pomeron exchange mechanism. By fixing the multi-pomeron exchange strength by the nuclear elastic scattering, the nuclear matter saturation and hypernuclear separation energies are reproduced in the G -matrix calculations, and the $2M_\odot$ neutron stars are found to be supported. In Ref. [24], the authors adopt a phenomenological hyperon-nucleon potential, which contains the ΛN forces consistent with the Λp scattering data and strongly repulsive Wigner type ΛNN force [25]. The Λ separation energies are well reproduced in the auxiliary field diffusion Monte-Carlo calculations, and the EOS fitted to the Monte-Carlo results can support the $2M_\odot$ neutron stars when the ΛNN forces are included [26]. In this treatment, the Λ separation energies in heavy Λ hypernuclei are calculated to be more than 60 MeV with the two-body ($2B$) forces, while they are reduced to be less than 30 MeV with the $3B$ forces. The effects of the $3B$ potential are very large, and it is natural to deduce that the four- and more baryon potential would be as important as the

$3B$ potential. In Ref. [27], internal structure modification of baryons is taken into account in the framework of the chiral quark meson coupling model. The modification leads to the σ dependence of the baryon- σ coupling, or the baryon- σ - σ multi-body coupling, where σ is the isoscalar scalar meson field. Because of the multi-body coupling and the Fock term contribution, hyperons are suppressed at high densities, and $2M_\odot$ neutron stars can be supported within the observation errors. While these approaches are successful in explaining the existence of $2M_\odot$ neutron stars with EOS including hyperons, it is preferable to derive the $3B$ interaction from a view point of the quark dynamics.

One of the possible origins of the $3B$ interaction is the determinant interaction of quarks, referred to as the Kobayashi-Maskawa-'t Hooft (KMT) interaction [28–31],

$$\mathcal{L}_{\text{KMT}} = g_D (\det \Phi + \text{h.c.}) , \quad (1)$$

$$\Phi_{ij} = \bar{q}_j (1 - \gamma_5) q_i , \quad (2)$$

where \det denotes the determinant with respects to the flavor indices, i and j . With three-flavors of quarks ($N_f = 3$), the KMT interaction replaces three quarks having different flavors with three quarks, then it can generate the $3B$ interaction; The $3B$ system having at least one u , d and s quarks can be connected by the KMT interaction as shown schematically in Fig. 1.

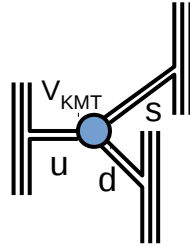


Fig. 1 Schematic picture of three-baryon interaction generated by the KMT interaction

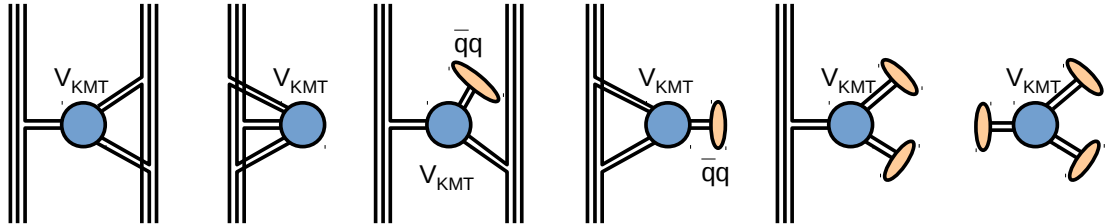


Fig. 2 Other interaction terms from the KMT interaction

The KMT interaction was introduced in order to account for the axial $U(1)$ ($U(1)_A$) anomaly [28, 29], and it was found to be generated by instantons [30, 31]. The strength of the KMT interaction g_D can be fixed by reproducing basic quantities of mesons. For

example, g_D was determined to be $g_D \Lambda^5 = -9.29$ [32] or $g_D \Lambda^5 = -12.36$ [33] in the Nambu–Jona-Lasinio (NJL) model [34, 35] by fitting the π , K and η' masses and the pion decay constant with other model parameters. Since the $U(1)_A$ anomaly pushes up the η' mass ($m_{\eta'}$), the value of g_D is essentially fixed by $m_{\eta'}$ [32].

From the above considerations, the $3B$ interaction from the KMT interaction has favorable features to resolve the hyperon puzzle. It acts only on systems including strange quarks, and it is probably repulsive because of the negative value of g_D . In the mean-field treatment for the NJL model, the KMT interaction pushes up the constituent quark mass [32], $M_u = m_u - 2g_s \langle \bar{u}u \rangle - 2g_D \langle \bar{d}d \rangle \langle \bar{s}s \rangle$, $M_d = m_d - 2g_s \langle \bar{d}d \rangle - 2g_D \langle \bar{s}s \rangle \langle \bar{u}u \rangle$, and $M_s = m_s - 2g_s \langle \bar{s}s \rangle - 2g_D \langle \bar{u}u \rangle \langle \bar{d}d \rangle$, where $m_{u,d,s}$ represents the current quark mass, g_s is the four-fermion scalar coupling, and $\langle \bar{q}q \rangle < 0$ is the quark condensate. The KMT interaction is found to act repulsively also in the $\Lambda\Lambda$ interaction [36]. While the color-magnetic interaction is strongly attractive in the flavor singlet six-quark state, the H dibaryon [37], the KMT interaction acts repulsively and the mass of H may be pushed up above the $\Lambda\Lambda$ threshold.

In this article, we discuss the $3B$ interaction generated by the KMT interaction in the quark cluster model. We adopt here the non-relativistic treatment for the wave functions of quarks and the KMT interaction. We consider the non-relativistic wave functions of quarks in baryons, and the spatial wave function is assumed to be $(0s)^3$; all quarks are assumed to be in the s -wave state of the harmonic oscillator potential and to have the same spatial extension. In the non-relativistic treatment of the KMT interaction, we ignore the γ_5 part in Φ_{ij} , then the KMT interaction becomes the zero-range three-body interaction among quarks (six-fermi interaction), which modifies the flavor but does not modify the spin and color of quarks.

This paper is organized as follows. In Sec. 2, we evaluate the norm of the one-, two-, and three-baryon wave functions in the quark cluster model. In Sec. 3, we quantify the $3B$ potential generated by the KMT interaction based on the three-baryon wave function and discuss its implication to the hyperon puzzle. Section 4 is devoted to the summary.

2. Quark cluster model wave function

2.1. One baryon state

We consider here the flavor-spin $SU(6)$ wave function of octet baryons. For example, the color, flavor, spin wave function for n_\uparrow , n_\downarrow and Λ_\uparrow are given as

$$\psi(n_\uparrow) = \frac{1}{\sqrt{3!}} \frac{1}{2\sqrt{3}} \varepsilon_{abc} [d_\uparrow d_\downarrow u_\uparrow + d_\downarrow d_\uparrow u_\uparrow - 2d_\uparrow d_\uparrow u_\downarrow]^{abc}, \quad (3)$$

$$\psi(n_\downarrow) = \frac{1}{\sqrt{3!}} \frac{1}{2\sqrt{3}} \varepsilon_{abc} [d_\downarrow d_\uparrow u_\downarrow + d_\uparrow d_\downarrow u_\downarrow - 2d_\downarrow d_\downarrow u_\uparrow]^{abc}, \quad (4)$$

$$\psi(\Lambda_\uparrow) = \frac{1}{\sqrt{3!}} \frac{1}{\sqrt{2}} \varepsilon_{abc} [u_\uparrow d_\downarrow s_\uparrow - u_\downarrow d_\uparrow s_\uparrow]^{abc}, \quad (5)$$

where ε_{abc} is the Levi-Civita tensor with respect to color indices. The first $1/\sqrt{3!}$ factor is the color symmetry factor, which is common to all baryons. The normalization factor is determined to normalize the fully antisymmetrized wave function, $\psi_A = \mathcal{A}/\sqrt{3!} \times \psi$. The antisymmetrizer \mathcal{A} is defined as

$$\mathcal{A}[q_1 q_2 \cdots q_n] = \sum_P \text{sgn}(P) q_{P(1)} q_{P(2)} \cdots q_{P(n)}, \quad (6)$$

Table 1 Octet baryon wave functions with the spin-up state. The fully antisymmetrized wave function is given as $|\psi_{\mathcal{A}}\rangle = \mathcal{A}/\sqrt{3!} \times \varepsilon_{abc}/\sqrt{3!} \times [|\text{Flavor}\rangle \otimes |\text{Spin}\rangle \otimes |\text{Spatial w.f.}\rangle]^{abc}$.

B	Flavor	Spin
n_{\uparrow}	$ ddu\rangle/\sqrt{2}$	$ \uparrow\downarrow\uparrow + \downarrow\uparrow\uparrow - 2\uparrow\uparrow\downarrow\rangle/\sqrt{6}$
p_{\uparrow}	$ uud\rangle/\sqrt{2}$	$ \uparrow\downarrow\uparrow + \downarrow\uparrow\uparrow - 2\uparrow\uparrow\downarrow\rangle/\sqrt{6}$
Λ_{\uparrow}	$ uds\rangle$	$ \uparrow\downarrow\uparrow - \downarrow\uparrow\uparrow\rangle/\sqrt{2}$
Σ_{\uparrow}^{-}	$ dds\rangle/\sqrt{2}$	$ \uparrow\downarrow\uparrow + \downarrow\uparrow\uparrow - 2\uparrow\uparrow\downarrow\rangle/\sqrt{6}$
Σ_{\uparrow}^0	$ uds\rangle$	$ \uparrow\downarrow\uparrow + \downarrow\uparrow\uparrow - 2\uparrow\uparrow\downarrow\rangle/\sqrt{6}$
Σ_{\uparrow}^{+}	$ uus\rangle/\sqrt{2}$	$ \uparrow\downarrow\uparrow + \downarrow\uparrow\uparrow - 2\uparrow\uparrow\downarrow\rangle/\sqrt{6}$
Ξ_{\uparrow}^{-}	$ ssd\rangle/\sqrt{2}$	$ \uparrow\downarrow\uparrow + \downarrow\uparrow\uparrow - 2\uparrow\uparrow\downarrow\rangle/\sqrt{6}$
Ξ_{\uparrow}^0	$ ssu\rangle/\sqrt{2}$	$ \uparrow\downarrow\uparrow + \downarrow\uparrow\uparrow - 2\uparrow\uparrow\downarrow\rangle/\sqrt{6}$

where P denotes permutation, q_i is the quark wave function, and $\text{sgn}(P)$ is the sign (or signature) of the permutation P . The flavor and spin wave functions for octet baryons are summarized in Table 1 for completeness.

The norm of the one baryon state is obtained as

$$\begin{aligned}
\mathcal{N}_{\mathcal{A}} &\equiv \langle \psi_{\mathcal{A}}(n_{\uparrow}) | \psi_{\mathcal{A}}(n_{\uparrow}) \rangle = \frac{1}{3!} \langle \mathcal{A}[\psi(n_{\uparrow})] | \mathcal{A}[\psi(n_{\uparrow})] \rangle = \langle \psi(n_{\uparrow}) | \mathcal{A}[\psi(n_{\uparrow})] \rangle \\
&= \frac{1}{3!} \sum_{i,j} c_i^* c_j \langle \varepsilon_{abc} \phi_i^{abc}(n_{\uparrow}) | \mathcal{A}[\varepsilon_{def} \phi_j^{def}(n_{\uparrow})] \rangle \\
&= \sum_{i,j} c_i^* c_j \langle \phi_i(n_{\uparrow}) | [\mathcal{S}_{\text{fss}} \phi_j(n_{\uparrow})]_{\text{fss}} \rangle = \sum_{i,j} c_i^* c_j \sum_P F_P(\phi_i, \phi_j) , \tag{7}
\end{aligned}$$

where $c_i = 1/2\sqrt{3}, 1/2\sqrt{3}, -1/\sqrt{3}$ ($i = 1, 2, 3$) and $\phi_i = d_{\uparrow}d_{\downarrow}u_{\uparrow}, d_{\downarrow}d_{\uparrow}u_{\uparrow}, d_{\uparrow}d_{\uparrow}u_{\downarrow}$ ($i = 1, 2, 3$) are the flavor-spin coefficient and component of the one-baryon wave function, respectively. The antisymmetrizer \mathcal{A} acts on the color, flavor, spin, and spatial coordinate wave functions, while the symmetrizer in the flavor-spin-spatial (fss) coordinates, \mathcal{S}_{fss} , does not exchange color indices. In the last line, the matrix element is obtained in the flavor, spin, and spatial coordinate wave functions, $F_P(\phi_i, \phi_j) = \langle \phi_i | P\phi_j \rangle_{\text{fss}}$. For example, one of the elements looks like

$$\begin{aligned}
\langle \phi_1(n_{\uparrow}) | [\mathcal{S}_{\text{fss}} \phi_2(n_{\uparrow})]_{\text{fss}} \rangle &= \sum_P F_P(\phi_1, \phi_2) \\
&= \langle d_{\uparrow}d_{\downarrow}u_{\uparrow} | d_{\downarrow}d_{\uparrow}u_{\uparrow} + d_{\uparrow}u_{\uparrow}d_{\downarrow} + u_{\uparrow}d_{\downarrow}d_{\uparrow} + d_{\downarrow}u_{\uparrow}d_{\uparrow} + u_{\uparrow}d_{\uparrow}d_{\downarrow} + d_{\uparrow}d_{\downarrow}u_{\uparrow} \rangle_{\text{fss}} = 1 , \tag{8}
\end{aligned}$$

provided that the spatial wave function is common to all quarks and normalized.

2.2. Two baryon states

Two-baryon states are defined as the product of two-baryon wave functions fully antisymmetrized in color, flavor, spin and spatial coordinates. We show the case of $n_{\uparrow}n_{\downarrow}$, as an example,

$$|\psi_{\mathcal{A}}(n_{\uparrow}, n_{\downarrow})\rangle = \frac{1}{\sqrt{6!}} |\mathcal{A}[\psi(n_{\uparrow})\psi(n_{\downarrow})]\rangle . \tag{9}$$

The norm of the above two-baryon state is obtained as

$$\begin{aligned}
\mathcal{N}_{\mathcal{A}} &= \langle \psi_{\mathcal{A}}(n_{\uparrow}, n_{\downarrow}) | \psi_{\mathcal{A}}(n_{\uparrow}, n_{\downarrow}) \rangle \\
&= \langle \psi(n_{\uparrow})\psi(n_{\downarrow}) | \mathcal{A}[\psi(n_{\uparrow})\psi(n_{\downarrow})] \rangle \\
&= \frac{1}{(3!)^2} \sum_{i,j,k,l} c_i^*(n_{\uparrow})c_j^*(n_{\downarrow})c_k(n_{\uparrow})c_l(n_{\downarrow}) \varepsilon_{abc} \varepsilon_{def} \varepsilon_{a'b'c'} \varepsilon_{d'e'f'} \\
&\quad \times \langle \phi_i^{abc}(n_{\uparrow})\phi_j^{def}(n_{\downarrow}) | \mathcal{A}[\phi_k^{a'b'c'}(n_{\uparrow})\phi_l^{d'e'f'}(n_{\downarrow})] \rangle \\
&= \sum_{i,j,k,l} c_i^*(n_{\uparrow})c_j^*(n_{\downarrow})c_k(n_{\uparrow})c_l(n_{\downarrow}) \sum_P C_P(\phi_i\phi_j, \phi_k\phi_l) F_P(\phi_i\phi_j, \phi_k\phi_l) , \quad (10)
\end{aligned}$$

The color and flavor-spin-spatial factors are shown by C_P and F_P . The exchange of quarks among baryons gives rise to a sign factor, which cannot be absorbed in the Levi-Civita tensor ε ,

$$\mathcal{A}[1^a 1^b 1^c 2^d 2^e 2^f] = 1^a 1^b 1^c 2^d 2^e 2^f - 1^a 1^b 2^d 1^c 2^e 2^f + 1^a 2^e 2^d 1^c 1^b 2^f + \dots , \quad (11)$$

where 1^a (2^d) shows one of the quarks in the first (second) baryon having the color index a (d). The color factor is obtained as the contraction of ε . For the case of the second term in Eq. (11), the first (second) three colors in the bra state need to be abd (cef) to have a finite matrix element, and we obtain

$$C_P = -\frac{1}{(3!)^2} \varepsilon_{abd} \varepsilon_{cef} \varepsilon_{abc} \varepsilon_{def} = -\frac{1}{36} 2\delta_{dc} 2\delta_{cd} = -\frac{1}{3} . \quad (12)$$

The color factor in the two-baryon case is found to be $C_P = 1, -1/3, 1/3, -1$ for zero, one, two and three quark exchanges between baryons, respectively. The flavor-spin-spatial factor for the permutation P is

$$F_P(\phi_i\phi_j, \phi_k\phi_l) = \langle \phi_i(n_{\uparrow})\phi_j(n_{\downarrow}) | P[\phi_k(n_{\uparrow})\phi_l(n_{\downarrow})] \rangle_{\text{fss}} = 0 \text{ or } 1 , \quad (13)$$

provided that two baryons are located at the same spatial point.

2.3. Three baryon states

Three-baryon states are defined in a way similar to the two-baryon states. For the $n_{\uparrow}n_{\downarrow}\Lambda_{\uparrow}$ state, the three-baryon wave function reads

$$| \psi_{\mathcal{A}}(n_{\uparrow}, n_{\downarrow}, \Lambda_{\uparrow}) \rangle = \frac{1}{\sqrt{9!}} | \mathcal{A}[\psi(n_{\uparrow})\psi(n_{\downarrow})\psi(\Lambda_{\uparrow})] \rangle . \quad (14)$$

The norm of three-baryon states are obtained as

$$\begin{aligned}
\mathcal{N}_{\mathcal{A}} &= \langle \psi_{\mathcal{A}}(n_{\uparrow}, n_{\downarrow}, \Lambda_{\uparrow}) | \psi_{\mathcal{A}}(n_{\uparrow}, n_{\downarrow}, \Lambda_{\uparrow}) \rangle \\
&= \langle \psi(n_{\uparrow})\psi(n_{\downarrow})\psi(\Lambda_{\uparrow}) | \mathcal{A}[\psi(n_{\uparrow})\psi(n_{\downarrow})\psi(\Lambda_{\uparrow})] \rangle \\
&= \frac{1}{(3!)^3} \sum_{i,j,k,l,m,n} c_{ijk}^*(n_{\uparrow}n_{\downarrow}\Lambda_{\uparrow})c_{lmn}(n_{\uparrow}n_{\downarrow}\Lambda_{\uparrow}) \varepsilon_{abc} \varepsilon_{def} \varepsilon_{ghi} \varepsilon_{a'b'c'} \varepsilon_{d'e'f'} \varepsilon_{g'h'i'} \\
&\quad \times \langle \phi_i^{abc}(n_{\uparrow})\phi_j^{def}(n_{\downarrow})\phi_k^{ghi}(\Lambda_{\uparrow}) | \mathcal{A}[\phi_l^{a'b'c'}(n_{\uparrow})\phi_m^{d'e'f'}(n_{\downarrow})\phi_n^{g'h'i'}(\Lambda_{\uparrow})] \rangle \\
&= \sum_{i,j,k,l,m,n} c_{ijk}^*(n_{\uparrow}n_{\downarrow}\Lambda_{\uparrow})c_{lmn}(n_{\uparrow}n_{\downarrow}\Lambda_{\uparrow}) \sum_P C_P(\phi_{ijk}, \phi_{lmn}) F_P(\phi_{ijk}, \phi_{lmn}) , \quad (15)
\end{aligned}$$

where $c_{ijk}(B_1 B_2 B_3) = c_i(B_1)c_j(B_2)c_k(B_3)$, $\phi_{ijk} = \phi_i\phi_j\phi_k$, and C_P and F_P are the color and flavor-spin-spatial factors, respectively.

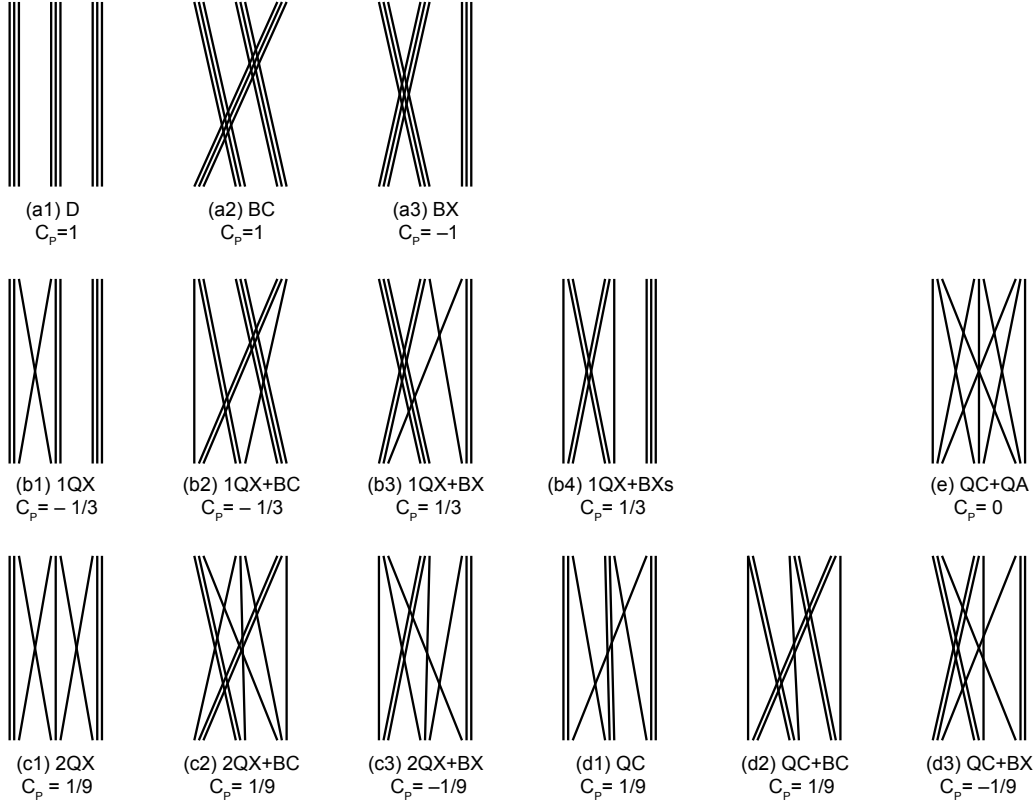


Fig. 3 Quark exchange diagrams and the corresponding color factor. See the text for the description of the quark exchanges.

Calculation of the color factor for the three-baryon states is straightforward but lengthy. We show one of the non-trivial examples,

$$\begin{aligned}
& -\frac{1}{(3!)^3} \varepsilon_{abc} \varepsilon_{def} \varepsilon_{ghi} \varepsilon_{a'b'c'} \varepsilon_{d'e'f'} \varepsilon_{g'h'i'} \langle 1^a 1^{b1} c^d 2^e 2^f 3^g 3^h 3^i \mid 1^{a'} 1^{b'} 3^{g'} 2^{d'} 3^{h'} 3^{i'} 1^{c'} 2^{e'} 2^{f'} \rangle \\
& = -\frac{1}{(3!)^3} \varepsilon_{abc} \varepsilon_{def} \varepsilon_{ghi} \varepsilon_{abg} \varepsilon_{dhi} \varepsilon_{cef} \langle 111222333 \mid 113233122 \rangle_{\text{fss}} \\
& = -\frac{1}{9} \langle 111222333 \mid 113233122 \rangle_{\text{fss}} . \tag{16}
\end{aligned}$$

In this case the color factor is $C_P = -1/9$.

Exchanges of quarks among three baryons can be categorized into the following types.

- (a1) Direct term (No quark exchange) (D).
- (a2) Cyclic baryon exchange (BC).
- (a3) Baryon exchange (BX).
- (b1) One quark pair exchange between two baryons (1QX).
- (b2) One quark pair exchange between two baryons after cyclic baryon exchange (1QX+BC).
- (b3) One quark pair exchange between two baryons after baryon exchange of the different baryon pair (1QX+BX).
- (b4) One quark pair exchange between two baryons after baryon exchange of the same baryon pair (1QX+BXs). (or two quark pair exchange between two baryons).

-
- (c1) Two quark pair exchange among three baryons with a stand baryon (2QX).
 - (c2) Two quark pair exchange among three baryons with a stand baryon after cyclic baryon exchange (2QX+BC).
 - (c3) Two quark pair exchange among three baryons with a stand baryon after baryon exchange (2QX+BX).
 - (d1) Cyclic three quark exchange (QC).
 - (d2) Cyclic three quark exchange after cyclic baryon exchange (QC+BC).
 - (d3) Cyclic three quark exchange after baryon exchange (QC+BX).
 - (e) Cyclic three-quark and anti-cyclic three-quark exchange among three baryons (QC+QA).

We schematically show the corresponding diagrams for these types in Fig. 3.

We find that the color factor is ± 1 when there is no quark exchange among baryons (a1, a2, a3). When one baryon keeps its three quarks (b1-b4), the color factor is $\pm 1/3$. In the case where all three baryons are involved in quark exchanges, the color factor is $\pm 1/9$ in most of the cases (c1-c3, d1-d3). The single exception is (e), $C_P = 0$, where the ket state is made of three baryons, each of which contains one quark from each baryon in the bra state. We summarize the color factor in Table 2, and the norm in some of two- and three-baryon systems in Table 3.

The norm of the three-baryon states can be more elegantly evaluated by using the reduction formula of the antisymmetrizer for the three octet-baryon states [38, 39],

$$\mathcal{A} = [1 - 9(P_{36} + P_{39} + P_{69}) + 27(P_{369} + P_{396}) + 54(P_{25} P_{39} + P_{35} P_{69} + P_{38} P_{69})] \mathcal{A}_B - 216 P_{25} P_{38} P_{69} , \quad (17)$$

$$\mathcal{A}_B = \sum_{\mathcal{P}} (-1)^{\pi(\mathcal{P})} \mathcal{P} , \quad (18)$$

where P_{ij} denotes the exchange operator of the i -th and j -th quark, P_{ijk} denotes the cyclic exchange operator of the ijk -th quarks, and \mathcal{P} is the baryon exchange operator. Equation (17) takes care of 1680 permutations, which act on $(3!)^3 = 216$ terms in the product of three antisymmetrized baryon wave functions and result in $1680 \times 216 = 9!$ permutations. In our categorization the first, second, third and fourth terms in the first line of Eq. (17) correspond to (a1-a3), (b1-b4), (d1-d3), and (c1-c3), respectively, and the second line corresponds to type (e).

3. Expectation value of the KMT operator and three-baryon potential

3.1. KMT operator and its expectation value

We now evaluate the KMT matrix elements in one-, two- and three-baryon systems. We concentrate on the $(0s)^6$ and $(0s)^9$ configurations of quarks for two- and three-baryon systems, respectively, which correspond to the cases where two- or three-baryons are located at the same spatial point.

In the non-relativistic treatment of the KMT interaction (2), we ignore terms which involve γ_5 and replace γ_0 with a unit matrix in Φ_{ij} ,

$$V_{\text{KMT}} \simeq -2g_D \int d^3x \varepsilon_{ijk} u^\dagger(\mathbf{x}) q_i(\mathbf{x}) d^\dagger(\mathbf{x}) q_j(\mathbf{x}) s^\dagger(\mathbf{x}) q_k(\mathbf{x}) . \quad (19)$$

Table 2 Color factor. See the text for the quark exchange.

Permutation	C_P	Type	Permutation	C_P	Type	
111 222 333	1	D (a1)	123 122 133	1/9		
222 333 111	1	BC (a2)	112 123 233	1/9	2QX (c1)	
333 111 222	1		113 223 123	1/9		
111 333 222	-1	BX (a3)	123 113 223	1/9	2QX+BC (c2)	
333 222 111	-1		133 123 122	1/9		
222 111 333	-1		233 112 123	1/9		
111 223 233	-1/3	1QX (b1)	123 233 112	1/9		
113 222 133	-1/3		223 123 113	1/9		
112 122 333	-1/3		122 133 123	1/9		
133 113 222	-1/3	1QX+BC (b2)	113 123 223	-1/9	2QX+BX (c3)	
333 112 122	-1/3		112 233 123	-1/9		
233 111 223	-1/3		123 133 122	-1/9		
223 233 111	-1/3		123 223 113	-1/9		
222 133 113	-1/3		233 123 112	-1/9		
122 333 112	-1/3		133 122 123	-1/9		
113 133 222	1/3	1QX+BX (b3)	123 112 233	-1/9	QC (d1)	
112 333 122	1/3		122 123 133	-1/9		
233 223 111	1/3		223 113 123	-1/9		
333 122 112	1/3		112 223 133	1/9		
223 111 233	1/3		113 122 233	1/9		
222 113 133	1/3		233 113 122	1/9		
111 233 223	1/3	1QX+BXs(b4)	133 112 223	1/9	QC+BC (d2)	
133 222 113	1/3		122 233 113	1/9		
122 112 333	1/3		223 133 112	1/9		
			112 133 223	-1/9		
			113 233 122	-1/9		
			133 223 112	-1/9		
		233 122 113	-1/9	QC+BX (d3)		
		223 112 133	-1/9			
		122 113 233	-1/9			
				123 123 123	0	QC+QA (e)

Then we obtain the matrix element of the KMT interaction for the three-quark states having a common color configuration as,

$$\begin{aligned}
& \langle q_1 q_2 q_3 | V_{\text{KMT}} | q'_1 q'_2 q'_3 \rangle \\
&= -2g_D \sum_{\{\alpha, \beta, \gamma\}} \int d^3x \varepsilon_{ijk} \langle q_\alpha | u^\dagger(\mathbf{x}) q_i(\mathbf{x}) | q'_\alpha \rangle \langle q_\beta | d^\dagger(\mathbf{x}) q_j(\mathbf{x}) | q'_\beta \rangle \langle q_\gamma | s^\dagger(\mathbf{x}) q_k(\mathbf{x}) | q'_\gamma \rangle \\
&= -2g_D \varepsilon_{ijk} \sum_{\{\alpha, \beta, \gamma\}} \langle q_\alpha | \hat{T}^{u,i} | q'_\alpha \rangle_{\text{fs}} \langle q_\beta | \hat{T}^{d,j} | q'_\beta \rangle_{\text{fs}} \langle q_\gamma | \hat{T}^{s,k} | q'_\gamma \rangle_{\text{fs}} \int d^3x \prod_\mu \varphi_\mu^*(\mathbf{x}) \varphi'_\mu(\mathbf{x}),
\end{aligned} \tag{20}$$

where the operator $\hat{T}^{i,j}$ replaces the flavor j with the flavor i , and $\varphi_\alpha(\mathbf{x})$ ($\varphi'_\alpha(\mathbf{x})$) shows the spatial part of the α -th quark wave function in the bra (ket) state. We find the quantum mechanical KMT interaction operator as,

$$V_{\text{KMT}} = -2g_{\text{D}}\varepsilon_{ijk} \sum_{\{\alpha,\beta,\gamma\}} \hat{T}_\alpha^{u,i} \hat{T}_\beta^{d,j} \hat{T}_\gamma^{s,k} \delta(\mathbf{x}_\alpha - \mathbf{x}_\beta) \delta(\mathbf{x}_\beta - \mathbf{x}_\gamma), \quad (21)$$

The operator $\hat{T}_\alpha^{i,j}$ now acts on the α -th quark. For more generic product wave functions with the same color configurations, $\phi = \prod_\alpha q_\alpha$ and $\phi' = \prod_\alpha q'_\alpha$, the KMT matrix element is found to be

$$\begin{aligned} \langle \phi | V_{\text{KMT}} | \phi' \rangle &= \sum_{\{\alpha,\beta,\gamma\}} \langle q_\alpha q_\beta q_\gamma | V_{\text{KMT}} | q'_\alpha q'_\beta q'_\gamma \rangle \prod_{i \neq \{\alpha,\beta,\gamma\}} \langle q_i | q'_i \rangle \\ &= -2g_{\text{D}} \langle \sigma | \sigma' \rangle \sum_{\{\alpha,\beta,\gamma\}} F_{\alpha\beta\gamma}^{\text{KMT}}(f, f') R_{\alpha\beta\gamma}^{\text{KMT}}(\varphi, \varphi'), \end{aligned} \quad (22)$$

$$\langle \sigma | \sigma' \rangle = \prod_\alpha \langle \sigma_\alpha | \sigma'_\alpha \rangle, \quad (23)$$

$$\begin{aligned} F_{\alpha\beta\gamma}^{\text{KMT}}(f, f') &= \langle f | \varepsilon_{ijk} \hat{T}_\alpha^{u,i} \hat{T}_\beta^{d,j} \hat{T}_\gamma^{s,k} | f' \rangle \\ &= \delta_{u,f_\alpha} \delta_{d,f_\beta} \delta_{s,f_\gamma} \sum_{ijk} \varepsilon_{ijk} \delta_{i,f'_\alpha} \delta_{j,f'_\beta} \delta_{k,f'_\gamma} \prod_{\mu \neq \{\alpha,\beta,\gamma\}} \delta_{f_\mu, f'_\mu}, \end{aligned} \quad (24)$$

$$\begin{aligned} R_{\alpha\beta\gamma}^{\text{KMT}}(\varphi, \varphi') &= \langle \varphi | \delta(\mathbf{x}_\alpha - \mathbf{x}_\beta) \delta(\mathbf{x}_\beta - \mathbf{x}_\gamma) | \varphi' \rangle \\ &= \int d^3x \varphi_\alpha^*(\mathbf{x}) \varphi_\beta^*(\mathbf{x}) \varphi_\gamma^*(\mathbf{x}) \varphi'_\alpha(\mathbf{x}) \varphi'_\beta(\mathbf{x}) \varphi'_\gamma(\mathbf{x}) \prod_{\mu \neq \{\alpha,\beta,\gamma\}} \langle \varphi_\mu | \varphi'_\mu \rangle. \end{aligned} \quad (25)$$

where σ_α , f_α and φ_α (σ'_α , f'_α and φ'_α) are the spin, flavor and spatial wave functions for the α -th quark in ϕ (ϕ'), respectively.

The KMT matrix elements in baryon systems are obtained as a sum of those for the product wave functions,

$$\begin{aligned} \mathcal{V}_{\mathcal{A}} &\equiv \langle \psi_{\mathcal{A}} | V_{\text{KMT}} | \psi'_{\mathcal{A}} \rangle = \langle \psi | V_{\text{KMT}} | \mathcal{A}[\psi'] \rangle = \sum_{I,J} c_I^* c_J \langle \phi_I | V_{\text{KMT}} | \mathcal{A}[\phi'_J] \rangle \\ &= -2g_{\text{D}} \sum_{I,J} c_I^* c'_J \sum_P C_P(\phi_I, \phi_J) \langle \sigma_I | P \sigma'_J \rangle \sum_{\{\alpha,\beta,\gamma\}} F_{\alpha\beta\gamma}^{\text{KMT}}(f_I, P f'_J) R_{\alpha\beta\gamma}^{\text{KMT}}(\varphi_I, P \varphi'_J), \end{aligned} \quad (26)$$

where c_I , f_I and φ_I (c'_J , f'_J and φ'_J) are the flavor-spin coefficients, flavor configurations, and spatial wave functions of the I -th (J -th) component of the baryon wave function in the bra (ket) state, respectively, and C_P is the color factor.

In Table 3, we show the norm and the diagonal matrix elements of the KMT operator,

$$\hat{\mathcal{T}}^{\text{KMT}} = \sum_{\{\alpha,\beta,\gamma\}} \varepsilon_{ijk} \hat{T}_\alpha^{u,i} \hat{T}_\beta^{d,j} \hat{T}_\gamma^{s,k}, \quad (27)$$

$$\begin{aligned} \mathcal{T}_{\mathcal{A}} &\equiv \langle \psi_{\mathcal{A}} | \hat{\mathcal{T}}^{\text{KMT}} | \psi_{\mathcal{A}} \rangle \\ &= \sum_{I,J} c_I^* c'_J \sum_P C_P(\phi_I, \phi_J) \langle \sigma_I | P \sigma'_J \rangle \sum_{\{\alpha,\beta,\gamma\}} F_{\alpha\beta\gamma}^{\text{KMT}}(f_I, P f'_J), \end{aligned} \quad (28)$$

in baryons sitting at $\mathbf{x} = 0$. Spatial wave functions are assumed to be the same for all quarks, then the norm becomes zero when the two baryons have the same flavors and spins.

Table 3 Norm and diagonal matrix elements of the KMT operator in two- and three-baryon systems of N and Λ . $2B$ and $3B$ matrix elements are evaluated by subtracting the contribution of subsystems (see text). For the one-baryon state, norm is unity and the KMT diagonal matrix element is zero.

Baryon(s)	\mathcal{N}_A	\mathcal{T}_A	\mathcal{T}	$\mathcal{T}_{nB}(n = 2, 3)$
$(NN)_{(S,T)=(0,1),(1,0)}$	10/9	0	0	0
$N_\uparrow\Lambda_\uparrow, N_\downarrow\Lambda_\downarrow$	1	20/3	20/3	20/3
$N_\uparrow\Lambda_\downarrow, N_\downarrow\Lambda_\uparrow$	1	10/3	10/3	10/3
$(\Lambda\Lambda)_{S=0}$	1	18/3	18/3	18/3
$(NNN)_{(S,T)=(1/2,1/2)}$	100/81	0	0	0
$n_\uparrow n_\downarrow \Lambda, p_\uparrow p_\downarrow \Lambda$	25/27	350/27	14	12/3
$n_\uparrow p_\uparrow \Lambda_\uparrow, n_\downarrow p_\downarrow \Lambda_\downarrow$	25/27	750/27	30	50/3
$n_\uparrow p_\uparrow \Lambda_\downarrow, n_\downarrow p_\downarrow \Lambda_\uparrow$	25/27	250/27	10	10/3
$n_\uparrow p_\downarrow \Lambda, n_\downarrow p_\uparrow \Lambda$	25/27	425/27	17	21/3
$N\Lambda_\uparrow\Lambda_\downarrow$	45/54	1035/54	23	21/3

For one-baryon states, the diagonal matrix elements of the KMT operator are found to be zero.

We have summed up the contributions of all the quark permutations, $3! = 6$, $6! = 720$ and $9! = 362880$ for one-, two-, and three-baryon(s), respectively. We note that $F_{\alpha\beta\gamma}^{\text{KMT}}$ is an integer, C_P is a multiple of $1/9$ and $c_I^* c_J'$ is a multiple of $(1/12)^{n-n_\Lambda} \times (1/2)^{n_\Lambda}$ for the diagonal matrix elements in n baryon systems with n_Λ being the number of Λ . Thus \mathcal{N}_A and \mathcal{T}_A are rational numbers. The genuine two- and three-baryon part of the matrix elements are evaluated by subtracting the contribution in subsystems. For example, for $n_\uparrow n_\downarrow \Lambda_\uparrow$ three-baryon systems, we subtract the $N\Lambda$ contributions,

$$\mathcal{T}_{3B}(n_\uparrow n_\downarrow \Lambda_\uparrow) = \mathcal{T}(n_\uparrow n_\downarrow \Lambda_\uparrow) - \mathcal{T}(n_\uparrow \Lambda_\uparrow) - \mathcal{T}(n_\downarrow \Lambda_\uparrow) = 4, \quad (29)$$

where $\mathcal{T} = \mathcal{T}_A/\mathcal{N}_A$.

We find that the expectation values of the KMT operator take positive values of $3 - 20$ for $2B$ and $3B$ systems including hyperons. Thus the KMT interaction is confirmed to generate a $3B$ repulsive potential when we have hyperons in $3B$ systems.

The expectation value of the KMT operator, \mathcal{T}_{2B} and \mathcal{T}_{3B} , is found to be spin-dependent: It is larger for larger spin states, for instance, $\mathcal{T}_{2B}((N\Lambda)_{S=1}) > \mathcal{T}_{2B}((N\Lambda)_{S=0})$ and $\mathcal{T}_{3B}((NN\Lambda)_{S=3/2}) > \mathcal{T}_{3B}((NN\Lambda)_{S=1/2})$. Since the KMT operator does not change the quark spin in the nonrelativistic treatment, more quark pairs have the same spin in the bra and ket and larger matrix element \mathcal{T}_A will appear in larger spin states. We note that the matrix element in the spin quartet state, $\mathcal{T}_{3B}((pn\Lambda)_{S=3/2})$, is much larger than others.

3.2. Baryon potentials from the KMT interaction

We evaluate the $3B$ potential from the KMT interaction (KMT-3B potential) as the expectation value of the $3B$ part of the KMT interaction operator (21) in three-baryons located

at $\mathbf{R}_1, \mathbf{R}_2$ and \mathbf{R}_3 ,¹

$$V_{3B}^{\text{KMT}}(\mathbf{R}_1, \mathbf{R}_2, \mathbf{R}_3) = \frac{\mathcal{V}_{\mathcal{A}}(\mathbf{R}_1, \mathbf{R}_2, \mathbf{R}_3)}{\mathcal{N}_{\mathcal{A}}(\mathbf{R}_1, \mathbf{R}_2, \mathbf{R}_3)} \Big|_{3B}, \quad (30)$$

where $\mathcal{V}_{\mathcal{A}}/\mathcal{N}_{\mathcal{A}}|_{3B}$ denotes the $3B$ potential part of the expectation value. The spatial part of the intrinsic baryon wave function is assumed to be $(0s)^3$; all quarks are assumed to be in the s -wave state of the harmonic oscillator potential and to have the same spatial extension,

$$\varphi_{\mathbf{R}}(\mathbf{x}) = \left(\frac{2\nu}{\pi}\right)^{3/4} \exp(-\nu(\mathbf{x} - \mathbf{R})^2), \quad (31)$$

where \mathbf{R} is the position of the baryon and the size parameter ν is related with the size of the quark wave functions b as $\nu = 1/(2b^2)$. The strength of the KMT matrix element for three baryons located at the same position ($\mathbf{R}_{1,2,3} = 0$) reads

$$V_{3B}^{\text{KMT}}(\mathbf{R}_{1,2,3} = 0) = -2g_{\text{D}}\mathcal{T}_{3B} \int d^3x \varphi_0(\mathbf{x})^6 = \frac{-2g_{\text{D}}}{(\sqrt{3}\pi b^2)^3} \mathcal{T}_{3B} = V_0 \mathcal{T}_{3B}. \quad (32)$$

By using the parameters, $g_{\text{D}}\Lambda^5 = -9.29$ and $\Lambda = 631.4$ MeV [32], $b = 0.6$ fm [40] or $b = 0.5562$ fm [41], we find

$$V_0 \equiv \frac{-2g_{\text{D}}}{(\sqrt{3}\pi b^2)^3} = \frac{-2g_{\text{D}}\Lambda^5}{(\sqrt{3}\pi b^2\Lambda^2)^3} \Lambda = \begin{cases} 1.45 \text{ MeV} & (b = 0.6 \text{ fm}), \\ 2.29 \text{ MeV} & (b = 0.5562 \text{ fm}). \end{cases} \quad (33)$$

If we take $g_{\text{D}}\Lambda^5 = -12.36$ and $\Lambda = 602.3$ MeV [33], V_0 becomes about 1.68 times larger than the values (33) because V_0 is linearly proportional to g_{D} . At finite $\mathbf{R}_{1,2,3}$, the spatial matrix element of the KMT operator is given as

$$\begin{aligned} R^{\text{KMT}} &\simeq \int d^3x \varphi_{\mathbf{R}_a}^*(\mathbf{x}) \varphi_{\mathbf{R}_b}^*(\mathbf{x}) \varphi_{\mathbf{R}_c}^*(\mathbf{x}) \varphi_{\mathbf{R}_d}(\mathbf{x}) \varphi_{\mathbf{R}_e}(\mathbf{x}) \varphi_{\mathbf{R}_f}(\mathbf{x}) \\ &= \frac{1}{(\sqrt{3}\pi b^2)^3} \exp\left[-\frac{\nu}{6} \sum_{i<j, i,j=a\sim f} \mathbf{R}_{ij}^2\right], \end{aligned} \quad (34)$$

where $\mathbf{R}_{ij} = \mathbf{R}_i - \mathbf{R}_j$ and $\mathbf{R}_i (i = a \sim f)$ is one of $\mathbf{R}_1, \mathbf{R}_2$ and \mathbf{R}_3 . When the antisymmetrization effects on the spatial wave function are ignored, other spatial matrix elements ($\prod \langle \varphi_{\mu} | \varphi'_{\mu} \rangle$ in Eq. (25)) cancels with those from the norm.² This prescription provides correct results when the baryons are separated enough or three-baryons are located at the same spatial point. The KMT-3B potential is then given as

$$V_{3B}^{\text{KMT}}(\mathbf{R}_1, \mathbf{R}_2, \mathbf{R}_3) \simeq V_0 \mathcal{T}_{3B} \exp\left[-\frac{2\nu}{3}(\mathbf{R}_{12}^2 + \mathbf{R}_{23}^2 + \mathbf{R}_{31}^2)\right]. \quad (35)$$

¹ Strictly speaking, this is the expectation value of the potential and not the potential itself. As long as the extension of the baryon wave function is large enough compared with the intrinsic extension of the quark wave function, however, the present treatment gives a good estimate of the potential.

² For a more serious discussion, we need to evaluate the spatial factor $R_{\alpha\beta\gamma}^{\text{KMT}}$ in Eq. (25) including the overlaps of other quarks, as well as those in the norm. In addition, the KMT matrix element can be finite also in those configurations having $\mathcal{T} = 0$ at zero distance. For example, the $n_{\uparrow}n_{\uparrow}\Lambda_{\uparrow}$ configuration has a zero norm and a zero KMT matrix element due to the Pauli blocking when three baryons are located at the same point, but will have a finite norm and a finite KMT matrix element at finite distances. These are beyond the scope of this paper, and we concentrate on the potentials in NNA and $N\Lambda\Lambda$ channels having finite KMT matrix elements at zero distance.

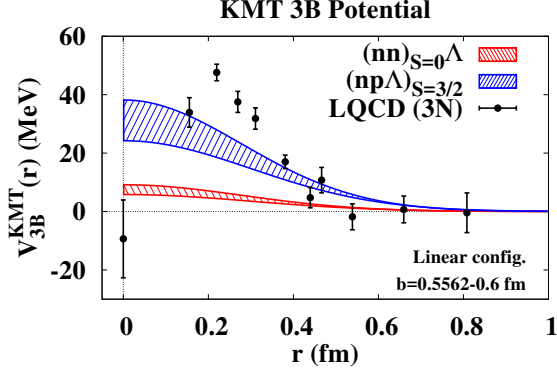


Fig. 4 Three-baryon potential in $(nn)_{S=0}\Lambda$ and $(np\Lambda)_{S=3/2}$ channels generated by the KMT interaction. Shaded area shows the uncertainties from the size parameter. Filled circles show the results of the $3N$ potential obtained in the lattice QCD simulation [23].

In Fig. 4, we show the KMT-3B potential V_{3B}^{KMT} for the NNA system in $(nn)_{S=0}\Lambda$ and $(np\Lambda)_{S=3/2}$ channels with a linear configuration in which three baryons are located at $\mathbf{R}_1 = (-r, 0, 0)$, $\mathbf{R}_2 = (0, 0, 0)$ and $\mathbf{R}_3 = (r, 0, 0)$. We adopt V_0 values evaluated in Eq. (33). The KMT- NNA potential at $r = 0$ has the height of 5.8 (9.2) MeV in $(nn)_{S=0}\Lambda$ channel and 24.2 (38.2) MeV in $(np\Lambda)_{S=3/2}$ channel for $b = 0.6(0.5562)$ fm, respectively, and the potential range is determined by the baryon size.

We compare the KMT- NNA potential with the $3N$ potential obtained by using the lattice QCD simulation (LQCD-3N potential) [23]. It is interesting to find that the KMT- NNA potential and the LQCD-3N potential have the same order of strengths and ranges, while the system is different and they do not need to agree. One of the differences is the short range behavior; the KMT- NNA potential has the peak at $r = 0$, whereas the LQCD-3N potential is suppressed at $r = 0$.

3.3. KMT-3B potential energy in nuclear matter

We shall now evaluate the KMT-3B potential energy per baryon in nuclear matter. We assume that the density of each baryons is constant, then we get the energy per baryon W_{3B}^{KMT} from the KMT-3B potential as

$$\begin{aligned}
 W_{3B}^{\text{KMT}} &= \frac{1}{\rho_B \Omega} \int d^3 R_1 d^3 R_2 d^3 R_3 \frac{1}{3!} \sum_{B_1, B_2, B_3} \rho(B_1) \rho(B_2) \rho(B_3) V_{3B}^{\text{KMT}}(B_1 B_2 B_3; \mathbf{R}_1, \mathbf{R}_2, \mathbf{R}_3) \\
 &= \frac{W_0}{3!} \left(\frac{\rho_B}{\rho_0} \right)^2 \sum_{B_1, B_2, B_3} \frac{\rho(B_1) \rho(B_2) \rho(B_3)}{\rho_B^3} \mathcal{T}_{3B}(B_1 B_2 B_3), \quad (36)
 \end{aligned}$$

$$W_0 = V_0 \left(\sqrt{3} \pi b^2 \right)^3 \rho_0^2 = -2g_D \rho_0^2 \simeq 0.28 \text{ MeV}. \quad (37)$$

where ρ_B is the baryon density and Ω denotes the spatial volume. It should be noted that W_0 is independent of the baryon size b . The KMT-3B potential energy per baryon in $n\Lambda$ matter is given as

$$W_{n\Lambda}^{\text{KMT}}(\rho_B, Y_\Lambda) = W_0 \left(\frac{\rho_B}{\rho_0} \right)^2 \left[\frac{1}{2} Y_n^2 Y_\Lambda \tilde{\mathcal{T}}_{3B}(NNA) + \frac{1}{2} Y_n Y_\Lambda^2 \tilde{\mathcal{T}}_{3B}(N\Lambda\Lambda) \right], \quad (38)$$

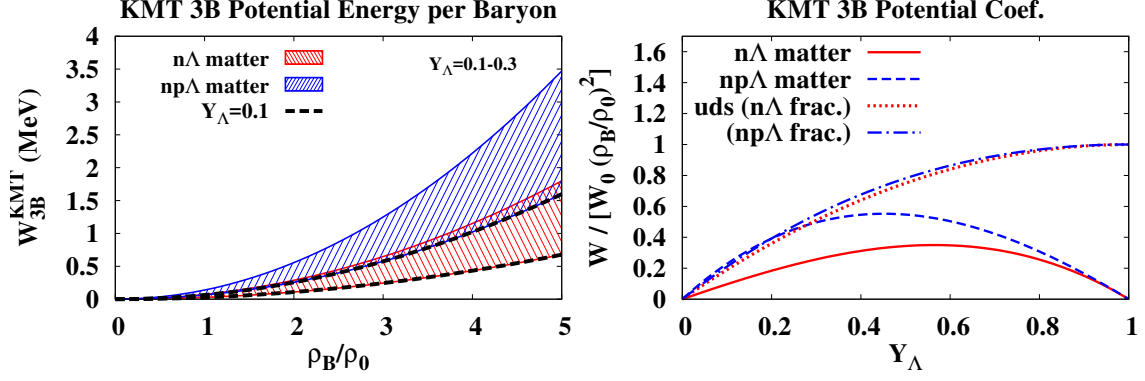


Fig. 5 KMT-3B potential energy per baryon in $n\Lambda$ and $np\Lambda$ matter (left), and the coefficients of the potential energy per baryon, $W^{\text{KMT}}/[W_0 (\rho_B/\rho_0)^2]$ in $n\Lambda$, $np\Lambda$ and quark matter (right).

where Y_n and Y_Λ represent the density fractions of n and Λ , $Y_n = \rho_n/\rho_B$ and $Y_\Lambda = \rho_\Lambda/\rho_B$, respectively, and $\tilde{\mathcal{T}}_{3B}(NNA)$ and $\tilde{\mathcal{T}}_{3B}(N\Lambda\Lambda)$ are the spin-averaged KMT matrix elements,

$$\tilde{\mathcal{T}}_{3B}(NNA) = \frac{1}{8} \sum_{\sigma_1, \sigma_2, \sigma_3} \mathcal{T}_{3B}(n_{\sigma_1} n_{\sigma_2} \Lambda_{\sigma_3}) = \frac{1}{2} \mathcal{T}_{3B}((nn)_{S=0}\Lambda) = 2, \quad (39)$$

$$\tilde{\mathcal{T}}_{3B}(N\Lambda\Lambda) = \frac{1}{8} \sum_{\sigma_1, \sigma_2, \sigma_3} \mathcal{T}_{3B}(N_{\sigma_1} \Lambda_{\sigma_2} \Lambda_{\sigma_3}) = \frac{1}{2} \mathcal{T}_{3B}(N(\Lambda\Lambda)_{S=0}) = \frac{7}{2}, \quad (40)$$

where $(S, T) = (0, 1)$ pair is taken for NNA . Note that $Y_n + Y_\Lambda = 1$ in $n\Lambda$ matter. For $np\Lambda$ matter, we find

$$W_{pn\Lambda}^{\text{KMT}}(\rho_B, Y_\Lambda) = W_0 \left(\frac{\rho_B}{\rho_0} \right)^2 \left[\frac{1}{2} (Y_n^2 + Y_p^2) Y_\Lambda \tilde{\mathcal{T}}_{3B}(NNA) + \frac{1}{2} (Y_n + Y_p) Y_\Lambda^2 \tilde{\mathcal{T}}_{3B}(N\Lambda\Lambda) + Y_n Y_p Y_\Lambda \tilde{\mathcal{T}}_{3B}(np\Lambda) \right], \quad (41)$$

where $\tilde{\mathcal{T}}_{3B}(np\Lambda)$ is the spin-averaged KMT matrix element in the $np\Lambda$ system,

$$\tilde{\mathcal{T}}_{3B}(np\Lambda) = \frac{1}{4} [\mathcal{T}_{3B}((np\Lambda)_{S=3/2}) + 2\mathcal{T}_{3B}(n_\uparrow p_\downarrow \Lambda) + \mathcal{T}_{3B}(n_\uparrow p_\uparrow \Lambda_\downarrow)] = \frac{17}{2}. \quad (42)$$

Note that $Y_n + Y_p + Y_\Lambda = 1$ in the $np\Lambda$ matter.

In the left panel of Fig. 5, we show the KMT-3B potential energy per baryon in $n\Lambda$ and $np\Lambda$ matter. Each shaded area corresponds to $0.1 \leq Y_\Lambda \leq 0.3$ and neutron and proton fractions are taken to be $Y_n = 1 - Y_\Lambda$ and $Y_n = Y_p = (1 - Y_\Lambda)/2$ for $n\Lambda$ and $np\Lambda$ matter, respectively. The KMT-3B potential energy per baryon amounts to be $W_{3B}^{\text{KMT}} = 0.027$ and 0.064 MeV at $(\rho_B, Y_\Lambda) = (\rho_0, 0.1)$ in $n\Lambda$ and $np\Lambda$ matter, respectively. At higher density and larger Λ fraction, the KMT-3B potential is found to reduce the nuclear symmetry energy slightly; $W_{3B}^{\text{KMT}} = 0.65$ and 1.25 MeV at $(\rho_B, Y_\Lambda) = (3\rho_0, 0.3)$ in $n\Lambda$ and $np\Lambda$ matter, respectively, then the KMT-3B potential reduces the difference of the energy per baryon in neutron matter with Λ admixture ($n\Lambda$ matter) and in symmetric nuclear matter with Λ admixture ($np\Lambda$ matter) by about 0.6 MeV.

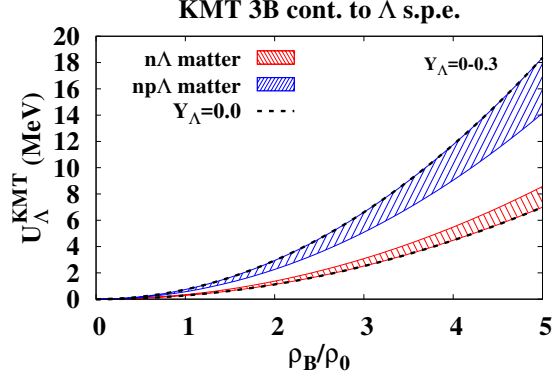


Fig. 6 KMT-3B potential contribution to Λ single particle energy.

It may be instructive to compare the above potential energy with that in quark matter having the same uds quark fractions,

$$W_{uds}^{\text{KMT}}(\rho_B) = W_0 \left(\frac{\rho_B}{\rho_0} \right)^2 Y_u Y_d Y_s , \quad (43)$$

$$Y_u = \rho_u/\rho_B = 2Y_p + Y_n + Y_\Lambda , \quad Y_d = Y_p + 2Y_n + Y_\Lambda , \quad Y_s = Y_\Lambda . \quad (44)$$

It should be noted that only the residual interaction contribution is considered here, and other contributions coming from the condensates are not counted. In the right panel of Fig. 5, we compare the coefficients of the potential energy per baryon, $W^{\text{KMT}}/[W_0(\rho_B/\rho_0)^2]$ in $n\Lambda$, $np\Lambda$ and quark matter. At small strange quark fraction (small Y_Λ), we note that the quark matter estimate agrees with the baryonic matter estimate in $np\Lambda$ matter, while baryonic matter estimate results in weaker KMT-3B repulsion in $n\Lambda$ matter.

Finally, we discuss the KMT-3B potential contribution to the Λ single particle energy,

$$U_\Lambda = \frac{\partial(\rho_B W)}{\partial \rho_\Lambda} . \quad (45)$$

In $n\Lambda$ and $pn\Lambda$ matter, we find

$$U_{\Lambda(n\Lambda)}^{\text{KMT}}(\rho_B, Y_\Lambda) = W_0 \left(\frac{\rho_B}{\rho_0} \right)^2 \left[\frac{1}{2} Y_n^2 \tilde{\mathcal{T}}_{3B}(NN\Lambda) + Y_n Y_\Lambda \tilde{\mathcal{T}}_{3B}(N\Lambda\Lambda) \right] , \quad (46)$$

$$U_{\Lambda(pn\Lambda)}^{\text{KMT}}(\rho_B, Y_\Lambda) = W_0 \left(\frac{\rho_B}{\rho_0} \right)^2 \left[\frac{1}{2} (Y_n^2 + Y_p^2) \tilde{\mathcal{T}}_{3B}(NN\Lambda) + (Y_n + Y_p) Y_\Lambda \tilde{\mathcal{T}}_{3B}(N\Lambda\Lambda) + Y_n Y_p \tilde{\mathcal{T}}_{3B}(np\Lambda) \right] , \quad (47)$$

In Fig. 6, we show the Λ single particle potential in $n\Lambda$ and $pn\Lambda$ matter. The neutron and proton fractions in $np\Lambda$ matter is again taken to be $Y_n = Y_p = (1 - Y_\Lambda)/2$. The average $pn\Lambda$ matrix element is larger than that of $nn\Lambda$, since we have more combinations of uds in $pn\Lambda$ matter. As a result, Λ feels more repulsion in symmetric matter than in pure neutron matter. The KMT-3B potential contribution to the Λ single particle energy is found to be $U_{\Lambda(n\Lambda)}^{\text{KMT}} \simeq 0.28$ MeV and $U_{\Lambda(pn\Lambda)}^{\text{KMT}} \simeq 0.73$ MeV at $\rho_B = \rho_0$ in neutron matter and symmetric nuclear matter ($n\Lambda$ and $pn\Lambda$ matter at $Y_\Lambda = 0$), respectively. These contributions are not large, but would be measurable in high-resolution experiments on the Λ separation energy of hyperisotopes such as ${}^{40}_{\Lambda}\text{K}$ and ${}^{48}_{\Lambda}\text{K}$ [42].

4. Summary

We have evaluated the expectation value of the determinant interaction of quarks, the Kobayashi-Maskawa [28, 29] and 't Hooft [30, 31] (KMT) interaction, in three-baryon systems, and have discussed the three-baryon potential from the KMT interaction. The KMT vertex gives rise to such three-quark interaction that all the u , d and s quarks need to participate. Then the KMT interaction is expected to generate potentials among three baryons which include at least one hyperon. The KMT interaction is responsible to the $U(1)_A$ anomaly, and its strength is determined from the η' mass [32, 33]. The negative sign of the strength parameter in the Lagrangian generates a repulsive three-quark interaction. Repulsive potential among three-baryons including hyperons may help to solve the hyperon puzzle of two-solar-mass neutron stars [1, 2].

The expectation value of the KMT operator (Eq. (27)) is obtained for the two- and three-baryon ($2B$ and $3B$) states consisting of nucleons and Λ baryons, where baryons are assumed to be located at the same spatial point. We have adopted nonrelativistic $(0s)^3$ wave functions for octet baryons, where a common spatial wave function is assumed for all quarks. $2B$ and $3B$ states are given as the product of baryon wave functions antisymmetrized under the quark exchanges. The KMT operator is found to take positive expectation values of 3 – 20 for $2B$ and $3B$ systems consisting of N and at least one Λ . Thus the KMT interaction is confirmed to generate $3B$ repulsive potential in $NN\Lambda$ and $N\Lambda\Lambda$ systems. The expectation value of the KMT operator, \mathcal{T}_{2B} and \mathcal{T}_{3B} , is found to be larger for the larger spin state, $\mathcal{T}_{2B}((N\Lambda)_{S=1}) > \mathcal{T}_{2B}((N\Lambda)_{S=0})$ and $\mathcal{T}_{3B}((NN\Lambda)_{S=3/2}) > \mathcal{T}_{3B}((NN\Lambda)_{S=1/2})$. Since the KMT operator does not change the quark spin in the nonrelativistic treatment, there can be more quark pairs having the same spin in the bra and ket of larger spin states and the expectation value of the KMT operator tends to be larger. We also note that the matrix element in the spin quartet state, $\mathcal{T}_{3B}((pn\Lambda)_{S=3/2})$, is much larger than others.

We have evaluated the $3B$ potential from the KMT interaction (KMT-3B potential). The strength of the $3B$ potential is calculated by using the harmonic oscillator wave function of quarks adopted in the quark cluster model analyses of $2B$ potentials [40, 41] and the strength of the KMT interaction obtained from the η' mass analyses [32]. The obtained $NN\Lambda$ potential from the KMT interaction has the height of 5.8 – 9.2 MeV in $(nn)_{S=0}\Lambda$ channel and 24.2 – 38.2 MeV in $(np\Lambda)_{S=3/2}$ channel at zero distance, and the potential range is determined by the baryon size. The strength and the range of the $3B$ potential in the linear configuration are found to be similar to those from the $3N$ potential obtained in the lattice QCD simulation [23] except the short range region.

The KMT-3B potential energy per baryon in nuclear matter W_{3B}^{KMT} and the KMT-3B potential contribution to the Λ single particle potential U_{Λ}^{KMT} are also estimated. The KMT-3B contribution to the equation of state, W_{3B}^{KMT} , is found to be small; $W_{3B}^{\text{KMT}} \simeq 0.05$ MeV and 0.1 MeV, for $n\Lambda$ and $np\Lambda$ matter at $(\rho_B, Y_{\Lambda}) = (\rho_0, 0.1)$, respectively. The KMT-3B contribution to the Λ single particle potential, U_{Λ}^{KMT} , is not large but would be visible; $U_{\Lambda}^{\text{KMT}} \simeq 0.56$ MeV and 1.2 MeV in $n\Lambda$ and $np\Lambda$ matter at $\rho_B = \rho_0$, respectively. The difference is small, but may be detectable in high-precision experiment on the separation energies of hyperisotopes such as ${}^{40}_{\Lambda}\text{K}$ and ${}^{48}_{\Lambda}\text{K}$ [42]. At $\rho_B = 3\rho_0$, U_{Λ}^{KMT} amounts to 2.5 MeV and 6.6 MeV in $n\Lambda$ and $np\Lambda$ matter, respectively. In order to solve the hyperon puzzle of massive

neutron stars, we need to find the mechanism to generate additional Λ single particle potential $\Delta U_\Lambda \sim 100$ MeV at around $\rho_B = 3\rho_0$, and the KMT-3B potential explains 2 – 7% of the required repulsion. Other three-quark interactions such as the confinement potential [43] can also contribute to the $3B$ potential.

Acknowledgments

This work was supported in part by the Grants-in-Aid for Scientific Research on Innovative Areas from MEXT (Nos. 24105008 and 24105001), Grants-in-Aid for Scientific Research from JSPS (Nos. 15K05079, 15H03663, 16K05349, 16K05350). K.M. was supported in part by the National Science Center, Poland under Maestro Grant No. DEC-2013/10/A/ST2/00106. K.K. was supported in part by Grant-in-Aid No. 26-1717 from JSPS.

A. Expectation values of KMT operator in one-, two-, and three-baryon systems

We have shown in Sec. 3 the expectation values of the KMT operator in some selected channels including N and Λ . In Fig. A1, we show the results for all states consisting of one-, two-, and three-octet baryons,

$$|\psi_{\mathcal{A}}\rangle = |B_\sigma\rangle, \quad \frac{\mathcal{A}}{\sqrt{6!}} |B_\sigma B'_{\sigma'}\rangle, \quad \frac{\mathcal{A}}{\sqrt{9!}} |B_\sigma B'_{\sigma'} B''_{\sigma''}\rangle. \quad (\text{A1})$$

Channels are sorted according to strangeness quantum number.

As already discussed in Ref. [39, 44], the norm takes small values in, for example, $(N\Sigma)_{(S,T)=(1,3/2)}$, $(\Xi^-\Xi^0)_{S=1}$ ($\mathcal{N}_{\mathcal{A}} = 2/9$) and $(N\Sigma^0)_{S=1}$, ($\mathcal{N}_{\mathcal{A}} = 13/27$), in $2B$ states,³ and $\Lambda(\Xi^-\Xi^0)_{S=1}$ ($\mathcal{N}_{\mathcal{A}} = 1/27$), $(nn)_{S=0}\Sigma^-$, $n(\Sigma^-\Sigma^-)_{S=0}$, $(pp)_{S=0}\Sigma^+$, $p(\Sigma^+\Sigma^+)_{S=0}$, $(\Xi^-\Xi^-)_{S=0}\Xi^0$, $\Xi^-(\Xi^0\Xi^0)_{S=0}$, ($\mathcal{N}_{\mathcal{A}} = 4/81$), in $3B$ states, where repulsion from the quark-Pauli effects is expected.

The expectation value of the KMT operator takes large values in, for example, $(\Lambda\Sigma)_{S=1}$ ($\mathcal{T} = 72/5$), $p_\uparrow\Xi_\downarrow^-$, $p_\downarrow\Xi_\uparrow^-$, $n_\uparrow\Xi_\downarrow^0$, $n_\downarrow\Xi_\uparrow^0$, $\Sigma_\uparrow^-\Sigma_\downarrow^+$, $\Sigma_\downarrow^-\Sigma_\uparrow^+$ ($\mathcal{T} = 288/23$), $(n\Sigma^-)_{S=1}$, $(p\Sigma^+)_{S=1}$, $(\Xi^-\Xi^0)_{S=1}$, ($\mathcal{T} = 12$), in $2B$ states, and $(\Sigma\Sigma\Sigma)_{S=3/2}$ ($\mathcal{T} = 584/11$), $(p\Lambda\Xi^-)_{S=3/2}$ ($n\Lambda\Xi^0)_{S=3/2}$ ($\mathcal{T} = 2374/47$), $p_\downarrow\Lambda_\uparrow\Xi_\uparrow^-$, $p_\uparrow\Lambda_\downarrow\Xi_\downarrow^-$, $n_\downarrow\Lambda_\uparrow\Xi_\uparrow^0$, $n_\uparrow\Lambda_\downarrow\Xi_\downarrow^0$ ($\mathcal{T} = 2106/46$), in $3B$ states. In some of $NN\Sigma$, $N\Lambda\Sigma$, $N\Sigma\Xi$, $N\Xi\Xi$, $\Lambda\Sigma\Sigma$, $\Sigma\Xi\Xi$, and $\Sigma\Sigma\Xi$ states, the $3B$ part of the expectation value is found to be negative, while \mathcal{T} is positive.

References

- [1] P. Demorest, T. Pennucci, S. Ransom, M. Roberts, and J. Hessels, *Nature*, **467**, 1081–1083 (2010), arXiv:1010.5788.
- [2] J. Antoniadis et al., *Science*, **340**, 6131 (2013), arXiv:1304.6875.
- [3] N. K. Glendenning and S. A. Moszkowski, *Phys. Rev. Lett.*, **67**, 2414–2417 (1991).
- [4] S. Nishizaki, T. Takatsuka, and Y. Yamamoto, *Prog. Theor. Phys.*, **108**, 703–718 (2002).
- [5] Z. H. Li and H. J. Schulze, *Phys. Rev.*, **C78**, 028801 (2008).
- [6] C. Ishizuka, A. Ohnishi, K. Tsubakihara, K. Sumiyoshi, and S. Yamada, *J. Phys.*, **G35**, 085201 (2008), arXiv:0802.2318.
- [7] K. Tsubakihara, H. Maekawa, H. Sumiyoshi, and A. Ohnishi, *Phys. Rev.*, **C81**, 065206 (2010), arXiv:0909.5058.
- [8] K. Masuda, T. Hatsuda, and T. Takatsuka, *Astrophys. J.*, **764**, 12 (2013), arXiv:1205.3621.
- [9] K. Masuda, T. Hatsuda, and T. Takatsuka, *PTEP*, **2013**(7), 073D01 (2013), arXiv:1212.6803.
- [10] L. Adamczyk et al., *Phys. Rev. Lett.*, **112**(16), 162301 (2014), arXiv:1401.3043.

³To describe $(N\Sigma)_{(S,T)=(0,1/2)}$ state having $\mathcal{N}_{\mathcal{A}} = 1/9$ or $(N\Lambda - N\Sigma)_{(S,T)=(0,1/2)}$ coupled state having $\mathcal{N}_{\mathcal{A}} = 0, 10/9$, off-diagonal matrix elements have to be accounted for.

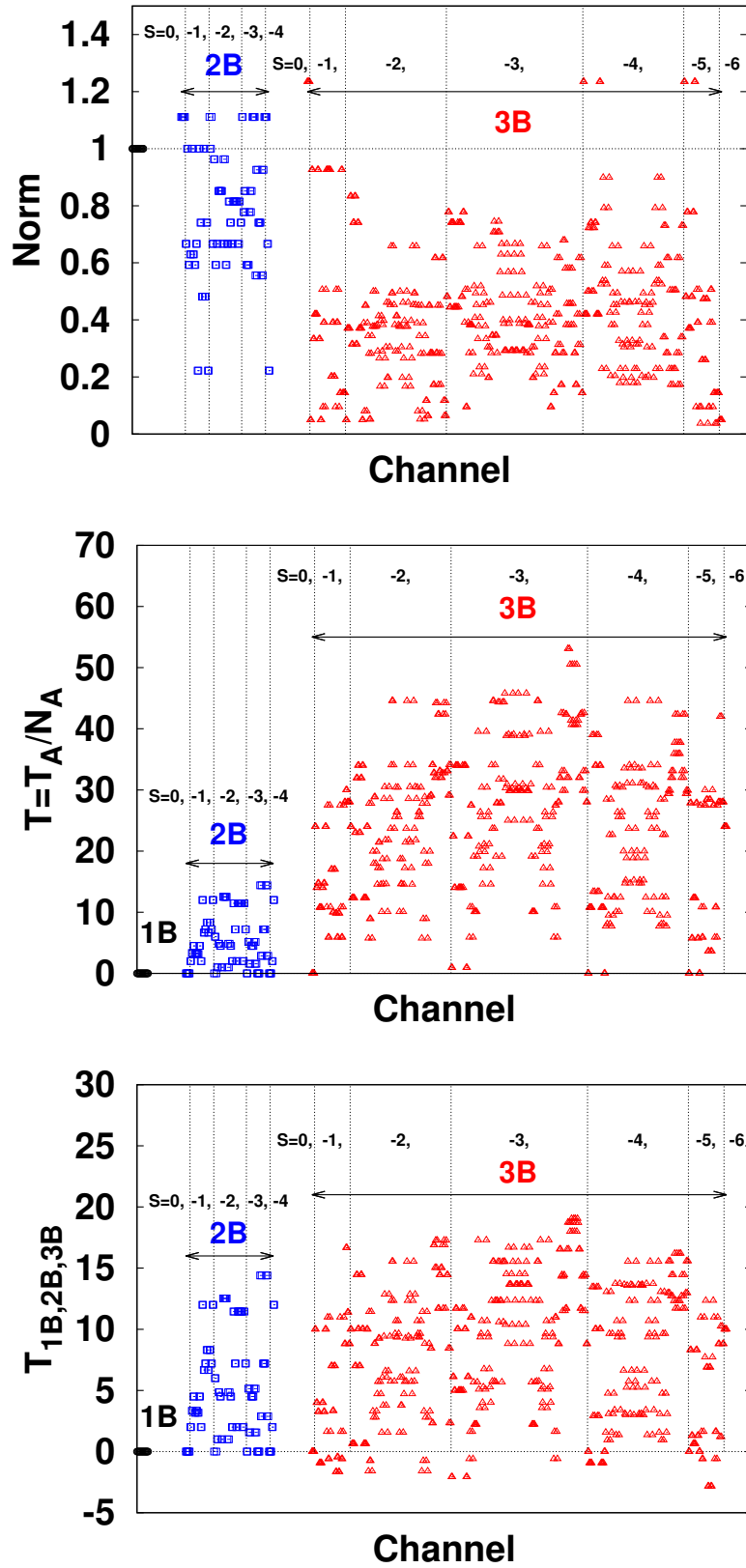


Fig. A1 Norm (top), expectation value of the KMT operator (middle) and its nB part (bottom) in one-, two-, and three-octet baryon states.

-
- [11] Y. Nara, H. Niemi, A. Ohnishi, and H. Stoecker, *Phys. Rev.*, **C94**(3), 034906 (2016), arXiv:1601.07692.
- [12] S. Weissenborn, D. Chatterjee, and J. Schaffner-Bielich, *Phys. Rev.*, **C85**(6), 065802, [Erratum: *Phys. Rev. C*90,no.1,019904(2014)] (2012), arXiv:1112.0234.
- [13] W. Freeman and D. Toussaint, *Phys. Rev.*, **D88**, 054503 (2013), arXiv:1204.3866.
- [14] J. Fujita and H. Miyazawa, *Prog. Theor. Phys.*, **17**, 360–365 (1957).
- [15] S. C. Pieper and R. B. Wiringa, *Ann. Rev. Nucl. Part. Sci.*, **51**, 53–90 (2001), arXiv:nucl-th/0103005.
- [16] Y. Yamamoto, T. Furumoto, N. Yasutake, and T. A. Rijken, *Phys. Rev.*, **C90**, 045805 (2014), arXiv:1406.4332.
- [17] E. Epelbaum, H.-W. Hammer, and U.-G. Meissner, *Rev. Mod. Phys.*, **81**, 1773–1825 (2009), arXiv:0811.1338.
- [18] R. Machleidt and D. R. Entem, *Phys. Rept.*, **503**, 1–75 (2011), arXiv:1105.2919.
- [19] B. Friedman and V. R. Pandharipande, *Nucl. Phys.*, **A361**, 502–520 (1981).
- [20] A. Akmal, V. R. Pandharipande, and D. G. Ravenhall, *Phys. Rev.*, **C58**, 1804–1828 (1998), arXiv:nucl-th/9804027.
- [21] M. Kohno, *Phys. Rev.*, **C88**(6), 064005 (2013), arXiv:1309.4556.
- [22] K. Sekiguchi, H. Sakai, W. H., W. Glöckle, J. Golak, M. Hatano, H. Kamada, H. Kato, Y. Maeda, J. Nishikawa, A. Nogga, T. Ohnishi, H. Okamura, N. Sakamoto, S. Sakoda, Y. Satou, K. Suda, A. Tamii, T. Uesaka, T. Wakasa, and K. Yako, *Phys. Rev.*, **65**, 034003 (2002).
- [23] T. Doi, S. Aoki, T. Hatsuda, Y. Ikeda, T. Inoue, N. Ishii, K. Murano, H. Nemura, and K. Sasaki, *Prog. Theor. Phys.*, **127**, 723–738 (2012), arXiv:1106.2276.
- [24] D. Lonardoni, F. Pederiva, and S. Gandolfi, *Phys. Rev.*, **C89**(1), 014314 (2014), arXiv:1312.3844.
- [25] A. R. Bodmer, Q. N. Usmani, and J. Carlson, *Phys. Rev.*, **C29**, 684–687 (1984).
- [26] D. Lonardoni, A. Lovato, S. Gandolfi, and F. Pederiva, *Phys. Rev. Lett.*, **114**(9), 092301 (2015), arXiv:1407.4448.
- [27] T. Miyatsu, S. Yamamuro, and K. Nakazato, *Astrophys. J.*, **777**, 4 (2013), arXiv:1308.6121.
- [28] M. Kobayashi and T. Maskawa, *Prog. Theor. Phys.*, **44**, 1422–1424 (1970).
- [29] M. Kobayashi, H. Kondo, and T. Maskawa, *Prog. Theor. Phys.*, **45**, 1955–1959 (1971).
- [30] G. 't Hooft, *Phys. Rev.*, **D14**, 3432–3450, [Erratum: *Phys. Rev. D*18,2199(1978)] (1976).
- [31] G. 't Hooft, *Phys. Rept.*, **142**, 357–387 (1986).
- [32] T. Hatsuda and T. Kunihiro, *Phys. Rept.*, **247**, 221–367 (1994), arXiv:hep-ph/9401310.
- [33] P. Rehberg, S. P. Klevansky, and J. Hufner, *Phys. Rev.*, **C53**, 410–429 (1996), arXiv:hep-ph/9506436.
- [34] Y. Nambu and G. Jona-Lasinio, *Phys. Rev.*, **122**, 345–358 (1961).
- [35] Y. Nambu and G. Jona-Lasinio, *Phys. Rev.*, **124**, 246–254 (1961).
- [36] S. Takeuchi and M. Oka, *Phys. Rev. Lett.*, **66**, 1271–1274 (1991).
- [37] R. L. Jaffe, *Phys. Rev. Lett.*, **38**, 195–198, [Erratum: *Phys. Rev. Lett.*38,617(1977)] (1977).
- [38] H. Toki, Y. Suzuki, and K. T. Hecht, *Phys. Rev.*, **C26**, 736–739 (1982).
- [39] C. Nakamoto and Y. Suzuki, *Phys. Rev.*, **C94**(3), 035803 (2016), arXiv:1606.07225.
- [40] M. Oka and K. Yazaki, *Prog. Theor. Phys.*, **66**, 572–587 (1981).
- [41] Y. Fujiwara, Y. Suzuki, and C. Nakamoto, *Prog. Part. Nucl. Phys.*, **58**, 439–520 (2007), arXiv:nucl-th/0607013.
- [42] F. Garibaldi et al., Jlab hypernuclear collaboration, conditionally approved experiment jlab c12-15-008. (2016).
- [43] T. T. Takahashi, H. Suganuma, Y. Nemoto, and H. Matsufuru, *Phys. Rev.*, **D65**, 114509 (2002), arXiv:hep-lat/0204011.
- [44] M. Oka, K. Shimizu, and K. Yazaki, *Nucl. Phys.*, **A464**, 700–716 (1987).